Engineering Geology 197 (2015) 267–277

Contents lists available at ScienceDirect

Engineering Geology

journal homepage: www.elsevier.com/locate/enggeo

Detection of uranium mill tailings settlement using satellite-based radar interferometry

Marius Necsoiu *, Gary R. Walter

Geosciences and Engineering Division, Southwest Research Institute®, San Antonio, Texas, United States

ARTICLE INFO

Article history:
Received 11 March 2015
Received in revised form 1 September 2015
Accepted 2 September 2015
Available online 7 September 2015

Keywords:
Earthen covers
InSAR
Measurement method
Mill tailings
Site analysis
Slope stability

ABSTRACT

The feasibility of monitoring erosion and settlement of earthen covers on uranium mill tailings impoundment was evaluated using synthetic aperture radar (SAR) coherence analysis, differential radar interferometry (DInSAR) and multi-temporal interferometry. A total of 13 ERS-1/-2 SAR images were acquired between August 22, 1996 and December 14, 2000 over two uranium mill tailings sites located in north-western New Mexico, USA. These SAR datasets were screened based on meteorological conditions at the time of acquisition, eliminating those acquired during (a) rain and thunderstorms, (b) mist or fog or, (c) during overcast conditions. Preliminary coherence analysis allowed us to better understand the dynamics of land disposal sites, to identify useful and relevant time domains and define the appropriate parameters for subsequent InSAR analyses. DInSAR allowed us to measure differential settlement of tens of mm over two 3 to 4 month periods. The Small BAseline Subset (SBAS) technique identified spatial variations in the rate of settlement ranging from approximately 1 mm/yr to 10 mm/yr. Although the extent of the analysis was limited by the availability of archived SAR data, the results demonstrated that monitoring using on-demand SAR data should yield reliable measurements of surface displacements earthen covers.

1. Introduction

Engineered earthen covers are used at land disposal sites to prevent or minimize releases of a variety of hazardous substances to the environment, such as radionuclides and hazardous organic and inorganic chemicals. The performance of the covers can be degraded by generalized or localized erosion (gully formation) and settlement of the underlying waste material (e.g., National Research Council, 1997). Standard methods of monitoring such covers and overall stability consist of visual inspection and may include elevation surveys of a few locations where tailings are settling, but site-wide elevation surveys to detect areas of ponding or incipient gully formation are not typically performed.

In recent years, radar interferometry or InSAR techniques have been recognized as an effective, low-cost technique for detecting and monitoring ground movements related to landslides, subsidence, and other natural hazards (e.g., Necsoiu and Hooper, 2009; Wasowski and Bovenga, 2014). Ideally low topography, no atmospheric artefacts and favourable environmental conditions (i.e., less vegetation, no snow cover, rain or overcast) allow radar signal coherence (e.g., radar phase) to be preserved between pairs of radar images over longer time intervals. In these conditions Differential Interferometric Synthetic Aperture Radar (DInSAR) could be successfully used to capture slow movements (cm/year). However, these conditions limited the use of DInSAR from a fully operational basis (Colesanti et al., 2003). Multi-temporal InSAR techniques, like Small BAseline Subset (SBAS) (Berardino et al., 2002), overcome some of DInSAR limitations. These techniques and their modifications are specifically designed to identify and quantify mm-level movement of area-based natural features (e.g., rock outcrops and boulders) and localized man-made structures (e.g., highway-related objects). The dimensions of the reflectors are usually smaller than the resolution cell and their coherence remains high for large temporal and geometrical bases. The SBAS technique exploits phase unwrapping by (1) assuming a certain type of correlation (similarity) between the movement of one pixel and that of the neighbouring ones and (2) making no assumptions on the type of movement (i.e., slow or fast and linear or nonlinear motions). These movements are equally well reconstructed by the SBAS algorithm, given that the spatial unwrapping step can be carried out.

A number of DInSAR studies documented the movements and settlement of underground mining sites (e.g., Stow and Wright, 1997; Herrera et al., 2007; Perski et al., 2009; Ng et al., 2010). Fewer multi-temporal InSAR studies focused in monitoring surface movement for open-pit mining (Wegmuller et al., 2007; Paradella et al., 2015), slope stability of waste piles (Pinto et al., 2014; Paradella et al., 2015), and tailing impoundments (Riedmann et al., 2013; Colombo, 2013). To our knowledge, the study presented here is the first that uses a combination of coherence, conventional and multi-temporal InSAR techniques focused on the stability of uranium mill tailing impoundments.

* Corresponding author.
E-mail address: mnecsoiu@swri.org (M. Necsoiu).

http://dx.doi.org/10.1016/j.enggeo.2015.09.002

The availability of satellite and digital elevation model (DEM) data, while essential, does not guarantee success in detecting line-of-sight displacement in a test area. Data coverage depends on the number of scatterers within the area of interest, which in part depends on ground conditions and the geometry of the satellite with respect to the ground target. In particular, the scatterer distribution is difficult to infer without significant data processing (for more on these issues please also see Wasowski and Bovenga, 2014). A major focus of this research was to determine if sufficient scatterers are present on the covers of uranium mill tailings impoundments to permit InSAR analyses.

2. Background

2.1. Site description

Two uranium mill tailings sites located in north-western New Mexico – the Bluewater site and the Grants Homestake site – were subjects of our investigation. The locations of these sites, along with the area covered by the SAR data, are shown in Fig. 1. Both sites are located in the Grants-Bluewater Valley on the northeast flank of the Zuni Mountains on the western edge of the San Juan sedimentary basin. The bedrock at the sites consists of Paleozoic and Mesozoic age carbonate and detrital formations and is covered with a veneer of recent basalt flows and alluvial deposits. The original land surface elevations are in the range of 1980 to 2010 m above mean sea level. The climate at both sites is semiarid with mean annual precipitation of 280 mm.

2.2. Bluewater tailings impoundment

The Bluewater main tailings impoundment was created by the processing of uranium ores at a mill operated by the Anaconda Company and then Atlantic Richfield Company (ARCO) between 1955 and 1982. The main tailings impoundment was covered by a radon and erosion barrier in 1995 as part of reclamation of the site (U.S. Department of Energy, 1997). Fig. 2 shows the topography of the main tailings impoundment after the cover was placed. The surface of the Main Tailings Impoundment is covered with 4.5 in. of rock, with a median diameter of 1.5 in.

The southern portion of the main tailings impoundment consists of predominantly sandy tailings and the northern portion consists of "slimes", which are very fine-grained materials from the processing of the uranium ore. The sandy portion of the tailings impoundment has a relatively steep topographic slope and the slimes portion has a very low topographic slope.

2.3. Grants (homestake) mill tailings impoundment

Homestake Mining Company operated a uranium mill at the Grants site from 1957 to 1990. A portion of the tailings from the milling operation was deposited in the large tailings impoundment (Fig. 3). The large tailings impoundment eventually rose to a height of approximately 30 m above the surrounding land. The sides of the large tailings impoundment are covered with at least 20 cm of basaltic rock, with a median diameter of not less than 12 cm (AK Geoconsult, 1993). Based on the latest data (i.e., October 1, 2014) Google Earth™ imagery, the surface of the impoundment is still undergoing modification and also may be undergoing continued settlement as water originally present in the tailings drains and by on-going extraction of pore water to control seepage.

3. Data and methods

A total of 13 ERS-1/ERS-2 SAR images, part from Track 141, Frame 2997 descending orbit mode, were selected and acquired through the Western North America interferometric synthetic aperture radar consortium (WInSAR). These SAR images were acquired between August 22, 1996 and December 14, 2000 (Table 1). These SAR datasets were selected from a larger pool and screened based on meteorological conditions at the time of acquisition, eliminating those acquired during (a) rain and thunderstorms, (b) mist or fog or, (c) during overcast conditions (Necsoiu et al., 2014). Datasets with large perpendicular baselines were also eliminated especially

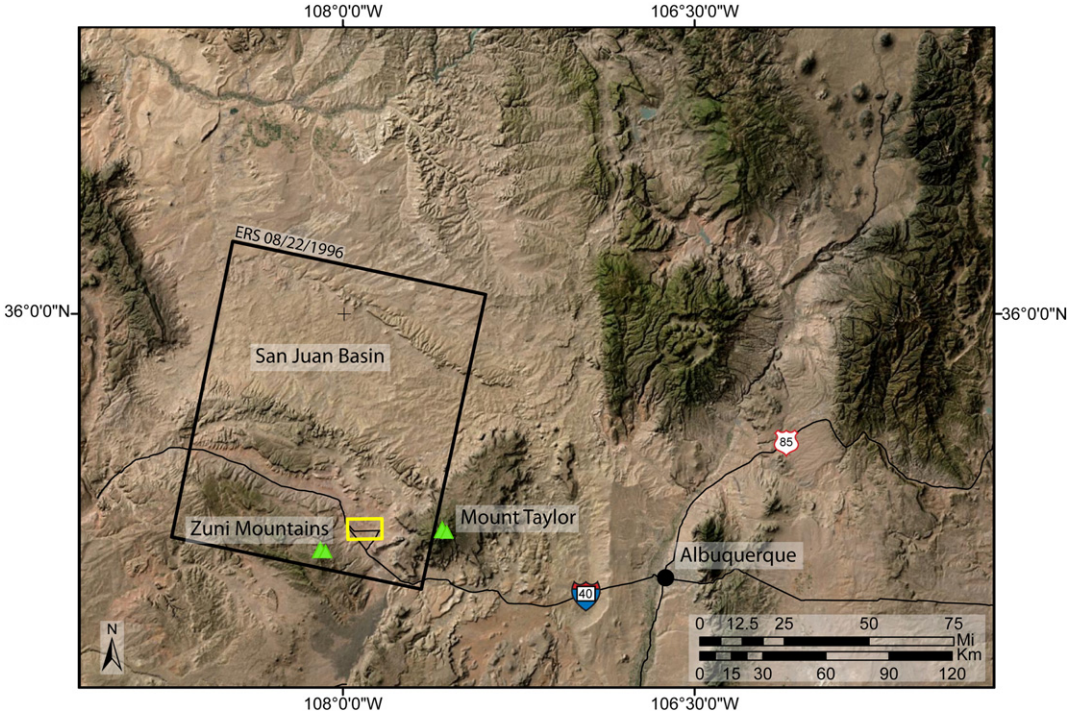

Fig. 1. Location of the study area (yellow rectangle, 133 sq. miles), ~90 miles West of Albuquerque, New Mexico. Black rectangle represents the extent of historical ERS-1/-2 SAR satellite data. Background is a natural colour pan-sharpened Landsat imagery, enhanced with topographic hillshading and colour balancing. Background image credit: USGS, NASA, ERSI Inc.

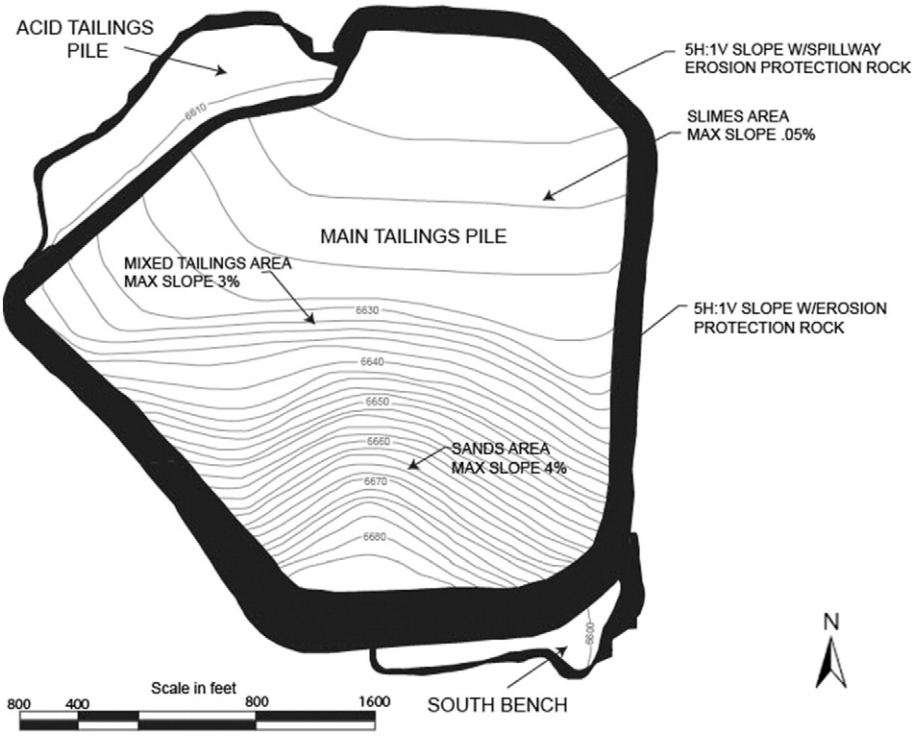

Fig. 2. As-built topography of the Bluewater main tailings pile area (U.S. Department of Energy, 1997).

when associated with atmospheric conditions as previously described. The spatial orientation of SAR acquisition corresponding to Track 141 allowed a good exposure of the Bluewater and a limited exposure (NE–SW is the less sensitive direction) of the Grants Homestake tailings impoundment slopes to the satellite line-of-sight, thus minimizing the geometrical effects induced by the side-

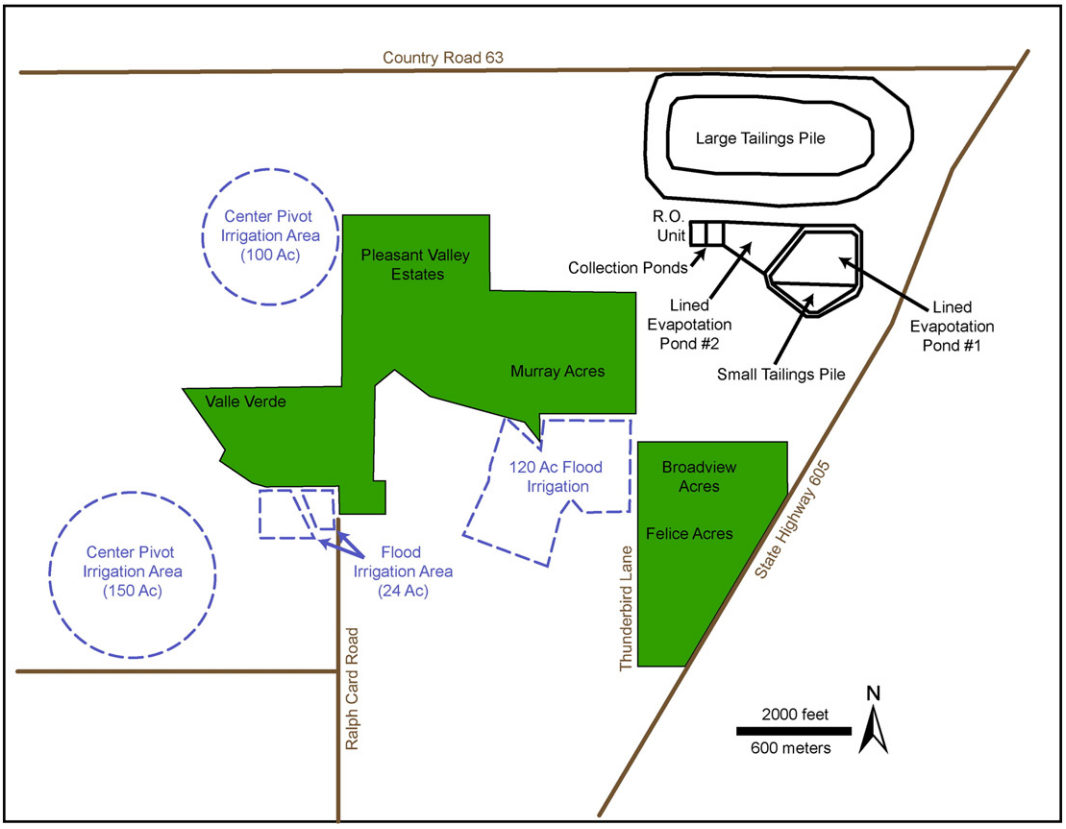

Fig. 3. Layout of the Homestake Grants Facility showing the large mill tailings impoundment (from http://www.nrc.gov/info-finder/decommissioning/uranium/is-homestake.pdf accessed May 13, 2014).

Table 1
SAR Data and the associated InSAR techniques.

Acquisition date	Normal baseline	SBAS(*) DInSAR(+)	
22-AUG 1996	−485.596	*	
05-DEC-1996	−359.456	*	
09-JAN-1997	238.398	*	+
13-FEB-1997	−109.088	*	
20-MAR-1997	−139.623	*	+
24-APR-1997	−181.268	*	
03-JUL-1997	0	*	
07-AUG-1997	292.948	*	
29-JAN-1998	174.987	*	
05-MAR-1998	−372.976	*	
09-APR-1998	−174.165	*	
31-AUG-2000	952.321		+
14-DEC-2000	862.183		+

looking geometry of SAR systems. To perform InSAR analyses, a 10-m DEM was produced based on a US Geological Survey National Elevation Dataset (NED). Data were re-projected to geographic coordinates with WGS84 datum.

Work was initiated by investigating the strength and coherence of the radar signal from the mill tailings covers. Qualitative analysis of coherence was used to assess how rapidly decorrelation of radar data occurred over the study sites. Specifically, rapid decorrelation is an indicator of highly dynamic ground displacements or changes in the environmental conditions of the target area. The results of the coherence analysis were used to select the best SAR image pairs for a quantitative DInSAR analysis and appropriate parameterization for SBAS InSAR analysis. A quality map based on mean coherence values (developed to identify areas permanently and temporary correlated), soil survey maps and field inspections assisted in selecting stable ground control

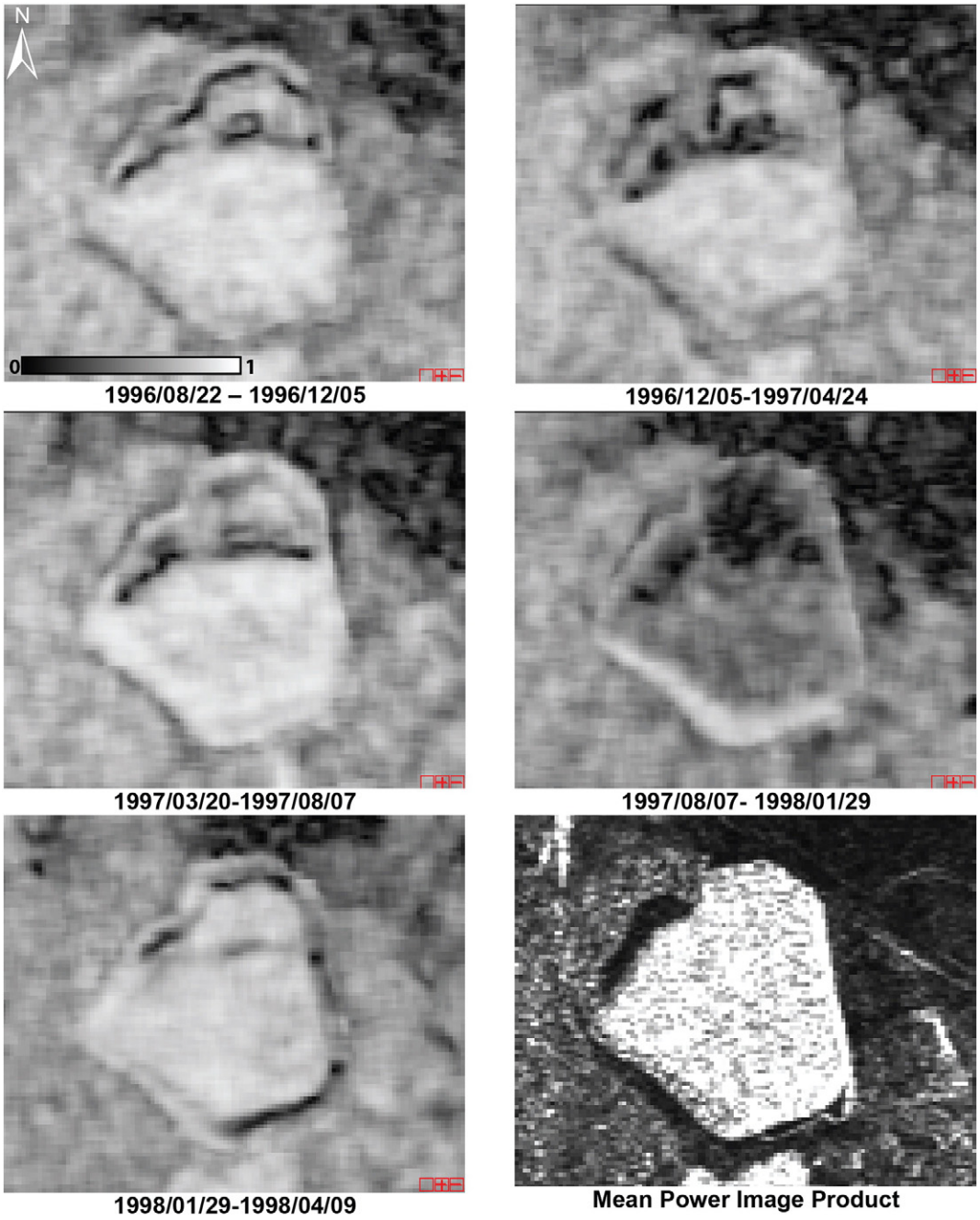

Fig. 4. Coherence analysis: SAR pairs showing nonlinear dynamics of the upper part of the Bluewater main tailings impoundment site. Data are presented in slant range geometry. Image chips are 2.4 km by 1.7 km.

points (GCPs) necessary to correct orbital inaccuracies of the input SAR datasets.

The multi-temporal InSAR processing followed a standard SBAS approach described in Berardino et al. (2002) and implemented in the SARscape software (Sarmap, 2014). Multi-looking factors for SAR datasets employed in range and azimuth was 1 respectively 5. The refinement and re-flattening step used initialization parameters from the orbital data and estimates based on the amplitude and coherence. Residual phase frequency was employed using a 512 × 512 window to eliminate those fringes which remained after the removal of the phase component, due to topography (i.e. DEM) and/or flat earth. A Goldstein approach (Baran et al., 2003) was used to flatten the initial interferograms and a minimum cost flow (MCF) algorithm was used in the unwrapping process. Unwrapped phase and coherence images were later used to identify and discard those InSAR pairs having large phase discontinuities and low coherence. These pairs were removed before the refinement and re-flattening step because their presence could significantly decrease the precision in the first velocity estimation. Finally the locations of 22 GCP points were used to improve displacement estimates by removing the atmospheric phase components and eventually fit a predefined displacement velocity model. GCPs were selected from flat areas (i.e., no evidence of residual topographic fringes), not be affected by any displacement, having high coherence over time and being spread all over the image.

In the first SBAS inversion step displacement related information (i.e., velocity, acceleration and acceleration variation) was estimated using a linear, quadratic and a cubic model, synthesized as follows:

$$\mathrm{Disp} = K + V^{*}(t\text{-}t_0) + 1/2\ A^{*}(t\text{-}t_0)^2 + 1/6\ \Delta A^{*}(t\text{-}t_0)^3 \quad (1)$$

Disp represents the displacement at time t relative to time t0; K is a constant term of order zero, which is used only for the final fitting process; V is the displacement velocity; A is the displacement acceleration; and ΔA is the acceleration variation.

The different nature of dynamics of those sites was captured by the chi-square parameter. Specifically, this parameter which quantifies the fit of the displacement time series was employed to quantify how well the output of the polynomial model (i.e., linear, quadratic and cubic,

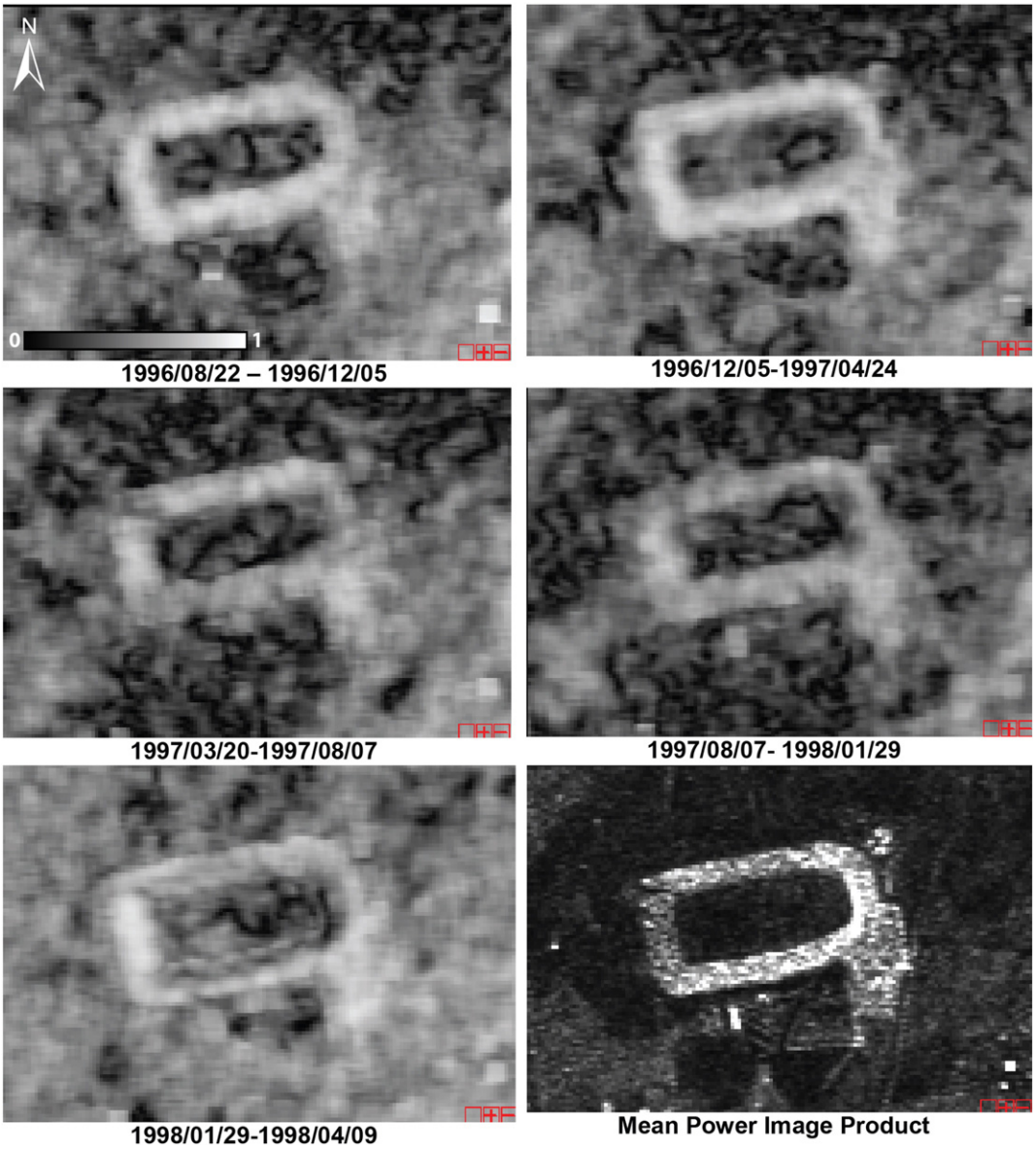

Fig. 5. Coherence maps based on selected SAR pairs showing consistently high values (low dynamics) on the slopes of the Grants Homestake site. Data are presented in slant range geometry. Image chips are 2.4 km by 1.7 km.

see Eq. (1)) fit/matches the measured displacement values. For each point location, the minimum value of chi-squares from linear, quadratic and cubic models was computed. This value was later used to select the most appropriate model to derive the final average displacement rate. In addition since only a small chi-square value appropriately represents the temporal behaviour of a time series, only those points with a threshold of 10 or less were selected.

SBAS InSAR provided the following information, in raster and vector formats:

- Average displacement rates (in mm/year, 20 m grid size)
- Coherence and total displacement (in mm, coherence threshold was set to 0.4)
- Displacement history, which consists of the displacement magnitude (in millimetres) for each input file with respect to the reference acquisition.

4. Results

4.1. Coherence

Figs. 4 and 5 present results based on the coherence analysis. Selected SAR pairs acquired a few months apart display lower coherence

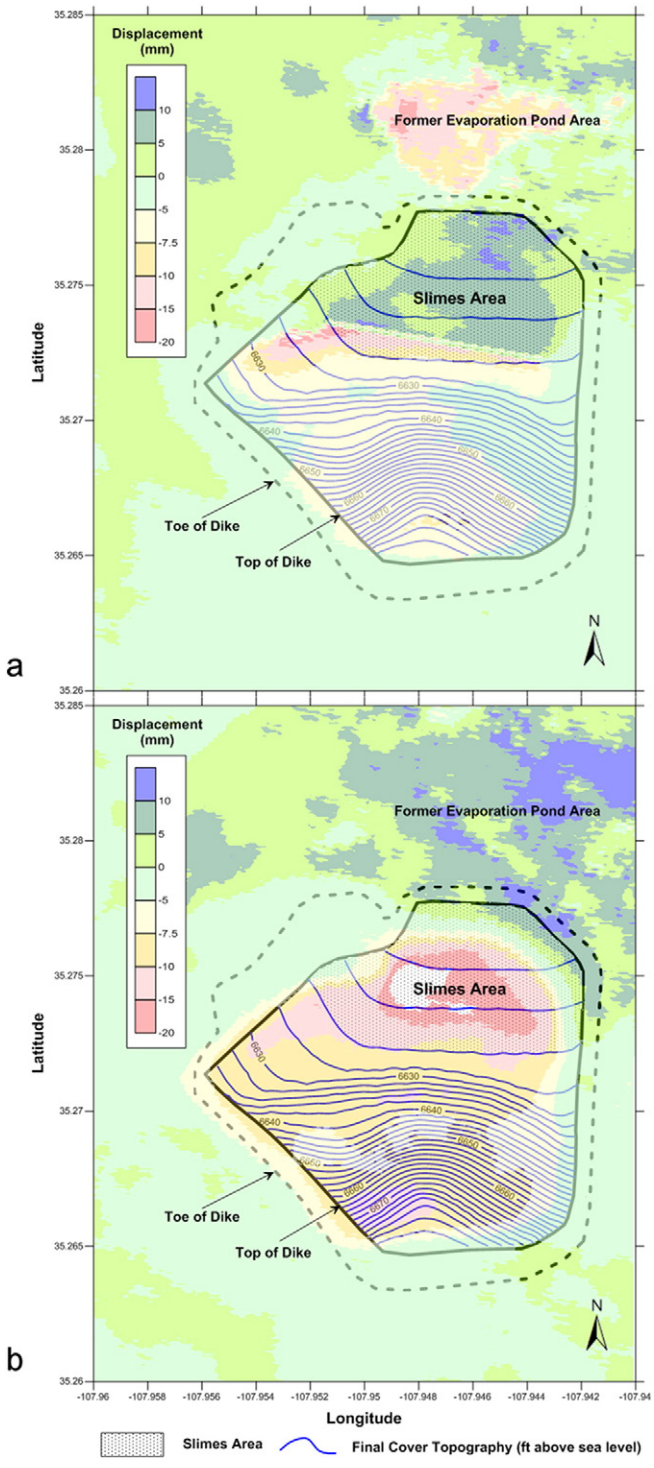

Fig. 6. Displacement of the cover of the Bluewater main tailings impoundment based on DInSAR analysis of SAR images for (a) 1997/01/09–1997/03/20, and (b) 2000/08/31–2000/12/14 along with surface elevation contours for the as-built cover.

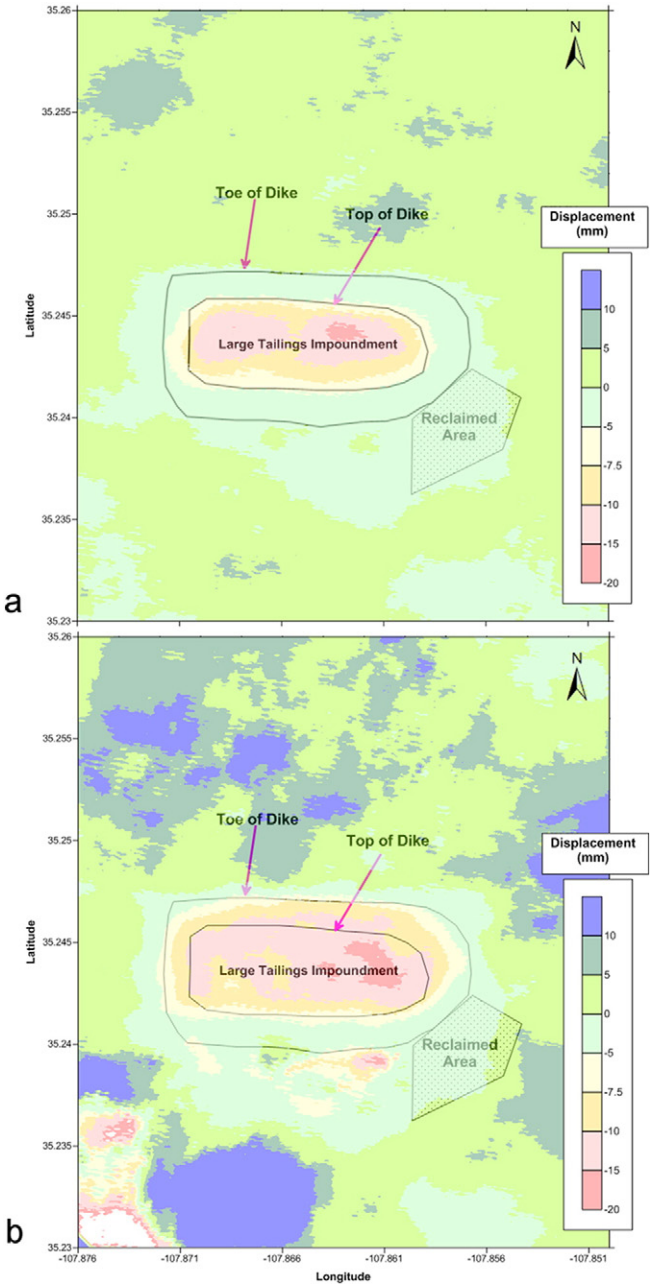

Fig. 7. Displacement of the cover of the Grants Homestake impoundment based on DInSAR analysis of SAR images for (a) 1997/01/09–1997/03/20, and (b) 2000/08/31–2000/12/14.

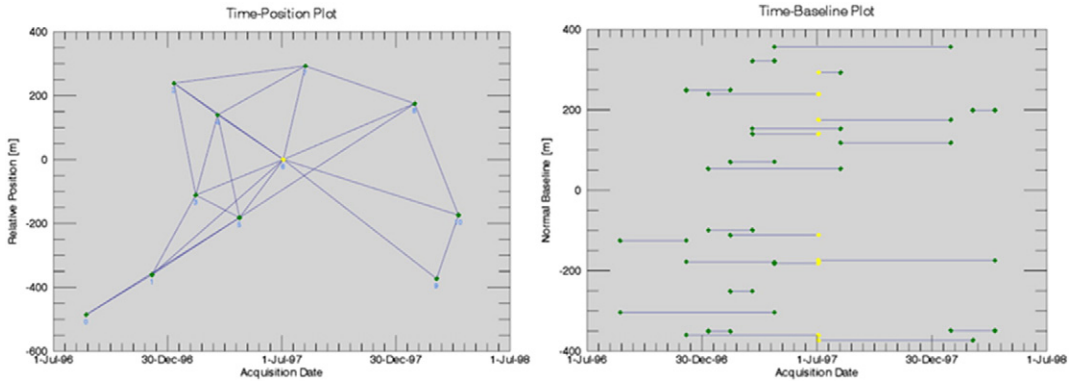

Fig. 8. Pairs (interferograms) processed of ERS-1/−2 SAR images processed by SBAS. Time versus relative position (on the left), and time versus normal baseline (on the right). One dataset acquired on 3 July 1997 (i.e., yellow dot in the graphs) had been chosen as the super master dataset.

(dark areas indicate lower coherence and possible greater dynamics) over the slime area of the Bluewater main tailings and active modification of the top of the Grants Homestake impoundment site. Mean power image products correspond to the mean intensity (digital number) calculated using all master images. They are used here mainly for visualization purposes, rough surfaces having higher intensity (i.e., bright values).

4.2. DInSAR

DInSAR requires that SAR data preserve coherence, which for the Bluewater and Grants sites required SAR data acquired no more than a few months apart. DInSAR was used to estimate displacements for data pairs acquired on January 9 and March 20, 1997, and on August 31 and December 14, 2000 (Figs. 6 and 7).

In Fig. 6a the DInSAR displacement patterns show a clear correlation with the slope of the mill tailings cover, with downward movements (negative displacements) over the steeper portion of the mill tailings underlain by relatively coarse tailings, and upward (positive displacements) over the slime area which contains primarily silt- and clay-sized tailings. A rapid change from downward to upward displacements occurs in the transition to the slimes disposal area. During the 2000 period (Fig. 6b), the slimes area moved down while the area with coarse tailings moved slightly up. Episodic seepage of water infiltrating through the area of coarse tailings into the slimes area with resulting changes in the pore pressure in the slime tailings may explain the dynamic behaviour of the slimes area.

The results of the DInSAR analyses for the Grants Homestake impoundment are shown in Fig. 7. The DInSAR analysis indicates the interior of the tailings impoundment was still undergoing settlement but the east, west, and north dike areas were relatively stable.

4.3. SBAS

SBAS analysis using a temporal baseline threshold of 6 months and a spatial baseline threshold of 40% of the critical baseline value was focused on 11 SAR images, acquired between August 22, 1996 and April 9, 1998. This analysis identified 7 master and 15 candidate SAR image pairs (Fig. 8). For each pair, the normal and temporal baselines were calculated. Overall, the mean, maximum, and minimum values are presented in Table 2.

Table 3 presents the number of points detected by the linear, quadratic and cubic displacement models. Specifically, in case of the Bluewater site, from 2333 SBAS point solutions, 2201 have the dynamic explained by one of these models, with 132 points having nonlinear dynamics not explained by any of these models. In the case of the Grants Homestake, all SBAS points, with exception of two locations, were explained by one of these models. Spatial distribution of these points for each of the site is presented in Fig. 9. The cubic model explained the dynamics for 78% of the Bluewater SBAS point locations and the quadratic model explained the dynamics for 67% of the Grants Homestake point locations. These models were selected in representing the final SBAS products with average displacement rates for Bluewater and Grants Homestake sites.

The results of the SBAS analysis for the Bluewater site are shown in Fig. 10. The graph (Fig. 10b upper right) shows the cumulative displacement of three selected points in and near the impoundment. Point 1 is located in the transition from the coarse tailings to the slimes. Point 2 is in the area of coarse tailings and Point 3 is outside the impoundment in an area that had little displacement. No SBAS points were generated in the slimes area due to its high and variable displacement dynamic. Based on the SBAS analysis, the coarse tailings area (Point 2) dropped by a total estimated displacement of approximately 10 mm over the 20 month period of analysis. This is generally consistent with the DInSAR displacements in the southern portion of the impoundment with downward movement. The total SBAS displacement of Point 1 in the transition between the coarse tailings and slime area was −30 mm, also consistent with the relative large displacement indicated by the DInSAR analysis.

Fig. 11 shows the results of the SBAS analysis for the Grants Homestake impoundment. SBAS displacements only could be generated for the side slopes of the impoundment and portions of the surrounding area. No SBAS displacements were generated on the surface of the impoundment because continued reclamation activities during the time period of the SBAS analysis degraded the coherence between the SAR data sets. The SBAS analysis indicates that the south dike (Points 1 and 2) is settling with respect to the east, west, and north dikes.

Although not a primary focus of this project, the area labelled as "Reclaimed Area" in Fig. 11 southeast of the impoundment generated many positive SBAS displacements that are consistent with the area of former uranium ore mill having been covered with clean fill. The absence of GCP in the immediate vicinity of both targeted sites (the closest GCPs were located at a distance of approximately 1 km) may have contributed to some of the noise in the SBAS results.

Table 2
Normal and temporal absolute baseline values.

Absolute baseline	Mean	Max	Min
Normal (m) (Critical value 937 m)	206.86	348.89	74.85
Temporal (days)	81	210	35

Table 3
Number of PS detected by three displacement models.

	Bluewater (2333 points)		Grants Homestake (1095 points)	
	Chi-square < = 10	Chi-square > 10	Chi-square < = 10	Chi-square > 10
Linear model	17	7	99	0
Quadratic model	463	28	729	0
Cubic model	1721	97	265	2

5. Discussion

Particular concerns that motivated this research were whether sufficient stable SAR scatterers would be present on the earthen covers to generate useful InSAR results and whether the existing SAR acquisitions could be close enough in time to preserve correlations in highly dynamic areas, such as rip rap covered surfaces. The coherence analysis provided a quick way to qualitatively detect areas that remain coherent over a long period of time. InSAR analyses provided a way to quantitatively assess rates of change for unstable areas. For the Bluewater site,

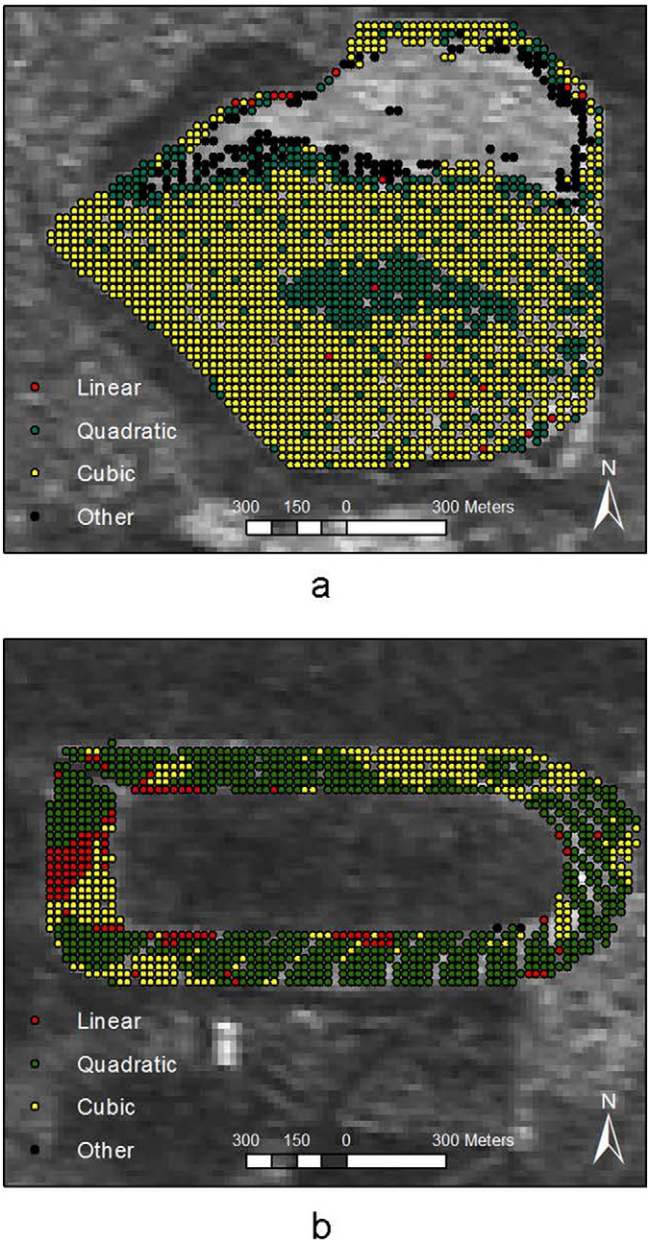

Fig. 9. Distribution of the minimum chi-square values of the linear, quadratic, cubic and unknown linear (other) models used in displacement estimates for (a) Bluewater main tailings site (b) Grants Homestake.

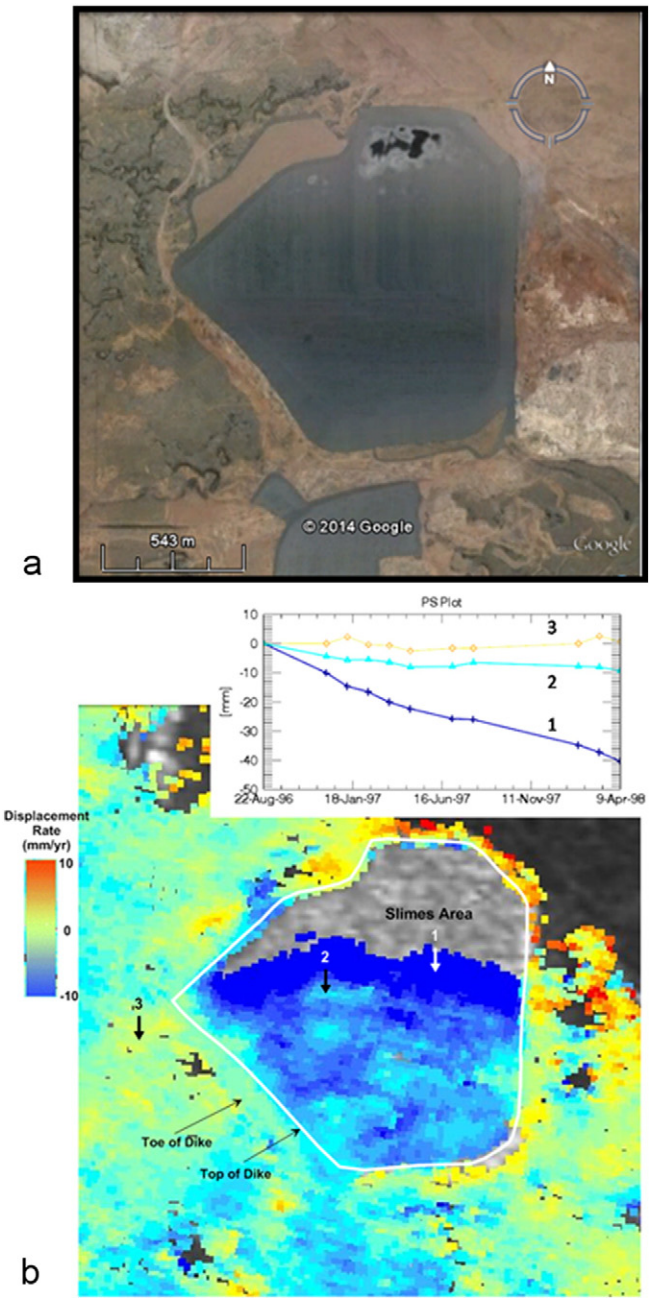

Fig. 10. (a) Bluewater main tailings site on an optical satellite image. (b) Average displacement rates and displacements of the cover of the Bluewater main tailings on SBAS analysis of SAR images from August 1996 through April 1998. The inserted graph shows the total displacement versus time at selected locations. No SBAS points were generated for the slimes area due to its high dynamics.

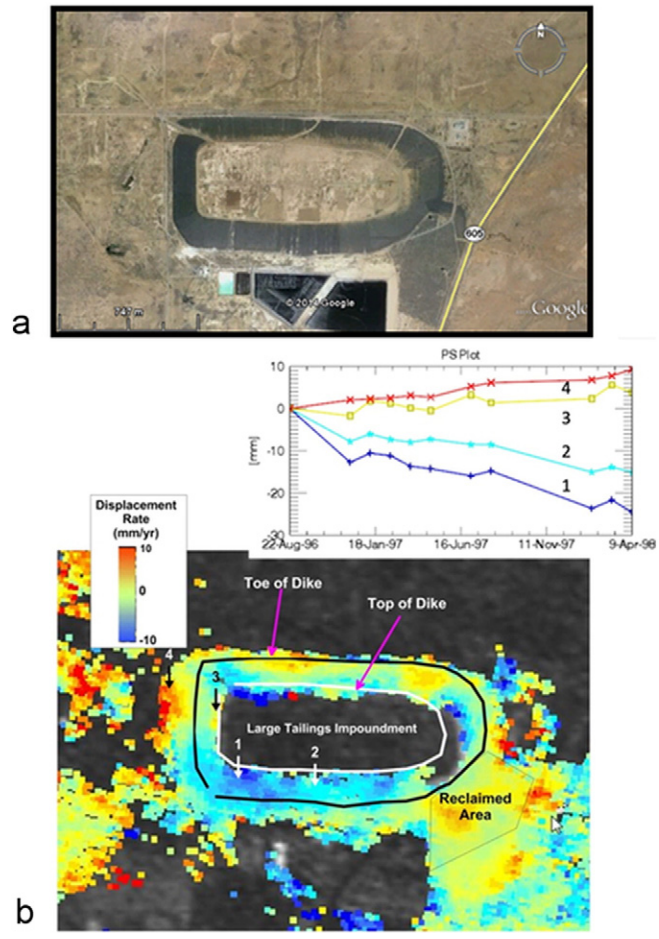

Fig. 11. (a) Grants Homestake Site on an Optical Satellite Image. (b) Average displacement rates and displacements of the Grants Homestake impoundment on SBAS analysis of SAR images from August 1996 through April 1998. The inserted graph shows the total displacement versus time at selected locations. No SBAS points were generated for the interior of the impoundment due to its high dynamics.

the DInSAR and SBAS analyses provided consistent centimetre-scale changes in ground surface displacements, mapped over the entire tailings impoundment. The displacements correlate with variations in the slope of the tailings impoundment cover and nature of the underlying tailings.

The SAR backscattering signal was relatively strong from both the Bluewater impoundment and the side dikes of the Grants Homestake impoundment. Both surfaces are covered with rock for erosion control. Whether or not similarly strong signals would be generated from covers using vegetation for erosion control is an open question. With regard to the effect of rip rap on temporal coherence, both sites generally preserved coherence over periods of 3 to 4 months. Loss of coherence over longer periods could be due to random displacements exceeding 1/2 wavelength of the SAR signal (2.8 cm) or other environmental factors. Although decorrelation limits the ability to perform quantitative InSAR analyses, loss of coherence can be a useful method for detecting large changes in landfill covers, such as large scale erosion and excessive settlement. The effects of decorrelation could be reduced using on demand SAR acquisitions with the time between acquisitions based on the correlation characteristics of the target site.

A relatively quick way to quantitatively assess the dynamics of these impoundments was to use DInSAR analysis based on a set of SAR images a priori selected from a coherence analysis. While SBAS leads to more accurate results than DInSAR, its displacement calculations are subject to a priori assumptions that may not accurately reflect the dynamics of the studied event, limiting its power to account for sudden, discontinuous changes. In the SBAS inversion step, a minimum-norm constraint on velocity is typically used (instead on the phase signal) which ultimately could filter-out high gradient data, to derive small discontinuities in the final solution. Therefore, episodic dynamics such as those identified in the northern part of the Bluewater site may be detected by the DInSAR analysis, but be excluded from the SBAS results based on the discontinuous displacement trajectory.

The SBAS results, while valid, contained only a subset of points for which the differences between the models output and the real dynamic of the area were small or negligible. Therefore, a coherence analysis executed early in the process can provide some hints on the type/range of the dynamics of the study area making a SBAS approach more or less appropriate for further quantitative investigations. The cubic model worked best for the Bluewater site and the quadratic model worked best for the Grants Homestake site, chi-square parameter proving to be useful for identifying those areas with different dynamic behaviours, not only in terms of high velocities, but also in terms of motion type (i.e., linear, quadratic, cubic, and unknown nonlinear).

Representing the SBAS average displacement rates of points, subject of different motion types (Figs. 10 and 11) was particularly challenging. To assess the differences in representing solutions of the linear and quadratic model versus the cubic model (as in case of Bluewater) and representing solutions of the linear and cubic model versus a quadratic model (as in case of the Grants Homestake), scatterplot analyses were further performed for each of these sites (Fig. 12). Overall, all the results show that the differences between the average displacement rates computed by these models were small, allowing any of the models to yield an acceptable representation of displacement rates. Analysis of the results shown in Fig. 12 yielded two additional observations. First, most of the points with linear solutions did not have solutions using the cubic and quadratic model (i.e., from 17 points only 5 had rate solutions computed by all three models). Second, a subpopulation of points (Fig. 12 b and d) had displacement rates calculated by the cubic model that were off-set (less negative) from those calculated using the quadratic model. That is, the cubic model yielded smaller settlement rates and higher uplift rates than the quadratic model. Further investigation revealed that all these points with off-set were located at the base of the slopes at each site. These points are better fit by the quadratic model in case of Bluewater site, which yields greater mean annual displacement values than the cubic model and in case of Grants site, by the cubic model which yields smaller mean annual displacement values than the quadratic model.

6. Conclusions

Although the InSAR analyses for this project were limited by the need to rely on archived SAR data, the results demonstrate that coherence analysis, DInSAR, and multi-temporal InSAR techniques (such as SBAS) can yield useful information on ground displacements occurring at uranium mill tailings impoundments and other land disposal sites with earthen covers. Future monitoring using on-demand SAR acquisitions with shorter revisiting times (e.g., the revisiting time of radar satellites has decreased from 35 days to 11 days with TerraSAR-X, 6 days for Sentinel-1 and 4 days with the COSMO-SkyMed satellite constellation, see also Table 1 in Wasowski and Bovenga, 2014) can yield reliable measurements of ground surface displacements, to guide maintenance of the cover. Because of intrinsic limitations (detection only in line-of-sight direction), complete characterization should involve field characterization. This work is also relevant to monitoring land disposal sites of other types of waste, waste rocks, and mine reclamation.

Acknowledgements

Funding for this work was provided by the Southwest Research Institute Nuclear Waste Management Internal Research and Development Project No. 20-8449. The authors thank Aaron Price and Sarah

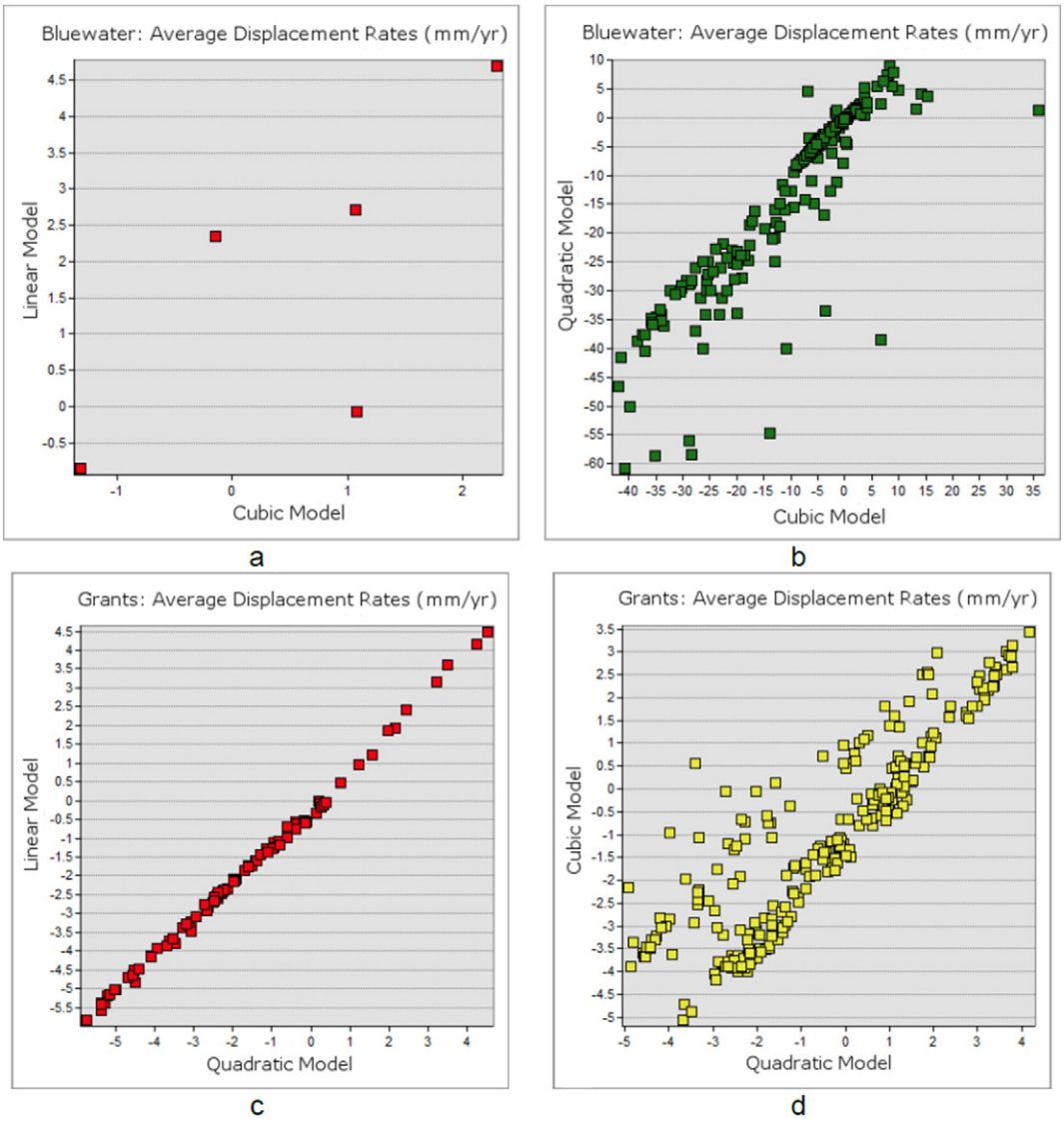

Fig. 12. Average displacement rates for PS detected by (a) a linear model and represented by a cubic model for Bluewater site (b) a quadratic model and represented by a cubic model for Bluewater site (c) a linear model and represented by a quadratic model for Grants site (d) a cubic model and represented by a quadratic model for Grants site.

Wigginton for their GIS assistance two anonymous reviewers for a critical and helpful review of this paper. SAR data were provided by the Western North America Interferometric Synthetic Aperture Radar (WInSAR) consortium; Soil survey maps were obtained from the Natural Resources Conservation Service Web Soil Survey, URL: http://websoilsurvey.nrcs.usda.gov.

References

AK Geoconsult, 1993. Reclamation plan, homestake mining company of California grants operation.

Baran, I., Stewart, M.P., Kampes, B.M., Perski, Z., Lilly, P., 2003. A modification to the Goldstein radar interferogram filter. IEEE Trans. Geosci. Remote Sens. 41 (9), 2114–2118.

Berardino, P., Fornaro, G., Lanari, R., Sansosti, E., 2002. A new algorithm for surface deformation monitoring based on small baseline differential SAR interferometry. IEEE Aerosp. Electron. 40 (11), 2375–2383.

Colesanti, C., Ferretti, A., Novali, F., Prati, C., Rocca, F., 2003. Monitoring of progressive and seasonal ground deformation. IEEE Trans. Geosci. Remote Sens. 41 (7), 1685–1701.

Colombo, D., 2013. Measuring deformation from space. InSAR as an operational tool for mining sector. web document, available at: http://www.ee.co.za/wp-content/uploads/2014/05/Davide-Colombo.pdf.

Herrera, G., Tomás, R., Lopez-Sanchez, J.M., Delgado, J., Mallorqui, J.J., Duque, S., Mulas, J., 2007. Advanced DInSAR analysis on mining areas: La Union case study (Murcia, SE Spain). Eng. Geol. 90 (3–4), 148–159. http://dx.doi.org/10.1016/j.enggeo.2007.01.001 (ISSN 0013-7952).

National Research Council, 1997. Barrier Technologies for Environmental Management, Summary of a Workshop. National Academy Press, Washington D.C.

Necsoiu, M., Hooper, D.M., 2009. Use of emerging InSAR and LiDAR remote sensing technologies to anticipate and monitor critical natural hazards. In: Fra Paleo, U. (Ed.), Building Safer Communities—Risk Governance, Spatial Planning and Responses to Natural Hazards. NATO Science for Peace and Security, Series E: Human and Societal Dynamics vol. 58, pp. 246–267. http://dx.doi.org/10.3233/978-1-60750-046-9-246.

Necsoiu, M., McGinnis, R.N., Hooper, D.M., 2014. New Insights on the Salmon Falls Creek Canyon Landslide Complex based on Geomorphological Analysis and Multitemporal Satellite InSAR techniques". Springer Berlin Heidelberg, Landslides, pp. 1141–1153 http://dx.doi.org/10.1007/s10346-014-0523-8 (11[6]).

Ng, A.H.-M., Ge, L., Yan, Y., Li, X., Chang, H.-C., Zhang, K., Rizos, C., 2010. Mapping accumulated mine subsidence using small stack of SAR differential interferograms in the Southern coalfield of New South Wales, Australia. Eng. Geol. 115 (1–2), 1–15. http://dx.doi.org/10.1016/j.enggeo.2010.07.004 (ISSN 0013-7952).

Paradella, W.R., Ferretti, A., Mura, J.C., Colombo, D., Gama, F.F., Tamburini, A., Santos, A.R., et al., 2015. Mapping surface deformation in open pit iron mines of carajás province (amazon region) using an integrated SAR analysis. Eng. Geol. 193, 61–78.

Perski, Z., Hanssen, R., Wojcik, A., Wojciechowski, T., 2009. InSAR analyses of terrain deformation near the Wieliczka Salt Mine, Poland. Eng. Geol. 106 (1–2), 58–67. http://dx.doi.org/10.1016/j.enggeo.2009.02.014 (ISSN 0013-7952).

Pinto, C.d.A., Paradella, W.R., Mura, J.C., Gama, F.F., Santos, A.R., Silva, G.G., 2014. Results of the application of persistent scatterers interferometry for surface displacements monitoring in the Azul open pit manganese mine (Carajás Province, Amazon region)

using TerraSAR-X data. Proc. SPIE 9245, Earth Resources and Environmental Remote Sensing/GIS Applications V, 92451 K http://dx.doi.org/10.1117/12.2067233.
Riedmann, M., Anderssohn, J., Lang, O., 2013. Monitoring of slope stability of tailings dams in South Africa using satellite interferometry. 2013 GRSG AGM — Status and Developments in Geological Remote Sensing.
Sarmap, 2014. SARscape user guide available at https://www.exelisvis.com/docs/pdf/sarscape_5.1_help.pdf.
Stow, R., Wright, P., 1997. Mining subsidence land surveying by SAR interferometry. 3rd ERS Symposium, Florence, Italy.
U.S. Department of Energy, 1997. Long-Term Surveillance Plan for the DOE Bluewater (UMTRCA Title II) Disposal Site Near Grants, New Mexico. U.S. Department of Energy Legacy Management, Washington, DC.
Wasowski, J., Bovenga, F., 2014. Investigating landslides and unstable slopes with satellite multi temporal interferometry: current issues and future perspectives. Eng. Geol. 174, 103–138. http://dx.doi.org/10.1016/j.enggeo.2014.03.003 (ISSN 0013-7952).
Wegmuller, U., Strozzi, T., Benecke, N., Petrat, L., Schlautmann, M., Kuchenbecker, R., Deutschmann, J., Spreckels, V., Schafer, M., Busch, W., Schade, M., Paar, W., Maly, R., Staisch, H., Hoffmann, F., Al-Enezi, A., 2007. Monitoring mining induced groundmovements using SAR interferometric techniques. Proceedings of ENVISAT Symposium, Montreaux, Switzerland, (ESA SP-636) (5 pp.)